American Mineralogist, Volume 87, pages 302–306, 2002

The crystal structure and cation ordering of Phase-X-$(K_{1-x-n})_2(Mg_{1-n}[Al,Cr]_n)_2Si_2O_7H_{2x}$: A potential K- and H-bearing phase in the mantle*

FRANCO MANCINI,[1,†] GEORGE E. HARLOW,[1] AND CHRISTOPHER CAHILL[2]

[1]Department of Earth and Planetary Sciences, American Museum of Natural History, Central Park West at 79th Street, New York, New York 10024-5192, U.S.A.

[2]Department of Chemistry, George Washington University, 725 21st Street, N.W. Washington, D.C. 20052, U.S.A.

ABSTRACT

Phase-X, a potassium di-magnesium acid disilicate, is a high-pressure synthetic compound—a potential K-bearing silicate in the mantle—with space group $P6_3cm$ (no. 185), $a = b = 5.028(2)$ Å, $c = 13.216(3)$ Å, $V = 289.34$ Å^3, $Z = 2$. The structure has been determined with 1521 CCD measured intensities and refined by the least-square method to $R = 0.0187$. The structure is built up of octahedral MgO sheets and layers containing disilicate groups, Si_2O_7, (with distinct Si1 and Si2 tetrahedra linked by the apical O2 atom) alternating along the **c** axis. The octahedral sheet is based on a hexagonal closest-packed array of two layers of non-equivalent O atoms, O1 and O3; two-thirds of all edge-sharing M octahedra are filled. Within the framework of the Si_2O_7 groups are channel structures parallel to [100], [010], and [110] that contain K atoms disordered in the middle of a large trigonal cavity (the A site). The FTIR spectrum in the OH stretching region shows a sharp peak at 3602 cm^{-1} due to OH^- ordered in one anion site; the position of hydrogen, which operates in a charge-balancing substitution for the partial occupancy of the A site $(K_{1-x}\square_x)^A \leftrightarrow H_x\square_{1-x})^H$, is undetermined. Densification in phase-X is affected by the greater compression of the empty octahedra in the octahedral layer and by constraining the trigonal A cavity containing the K atom to the size of the Si_2O_7 disilicate group. This dense packing contributes to the relatively high zero-pressure calculated density of 3.38 g/cm^3.

INTRODUCTION

Potassium plays an important role in the Earth as a result of its involvement in differentiation, its preferred partitioning into partial melts, and its contribution to the heat budget of the Earth by means of radioactive decay of ^{40}K. More recently, it has also been found to be influential in melting of the Earth's mantle because the phases in which it is commonly hosted (e.g., phlogopite and amphibole) are key to dehydration melting. Thus, determination of phases that are potential sinks for potassium at high pressure is likewise important. The K-bearing phases stable at high pressure include phlogopite, sanidine, K-cymrite (e.g., Fasshauer et al. 1997; Thompson et al. 1998), KK-richterite (e.g., Ulmer and Konzett 1999; Konzett and Fei 2000), K-hollandite (Yamada et al. 1984; Schmidt 1996; Irifune et al. 1994) and K-rich clinopyroxene (see Harlow 1997); several of these are hydrous as well. Phase-X was discovered in synthesis products in various studies (Trønnes 1990; Harlow 1997; Luth 1997; Inoue et al. 1998; Ulmer and Konzett 1999; Konzett and Fei 2000) at a range of conditions from $T = 1150$–1400 °C and $P = 9$–17 GPa, which makes it a potential host for K and H_2O at mantle conditions. Measured compositions of phase-X are high in K_2O (10–15 wt%) and MgO (26–39 wt%) and low in Al_2O_3 (e.g., Konzett and Fei 2000), although no systematic studies of compositional range have yet been undertaken. With the interpreted ideal stoichiometry of Konzett and Fei (2000), $K_{2-x}Mg_2Si_2O_7H_x$, it can incorporate a significant amount of hydrogen, which as H_2O ranges from 1.8–4.2 wt%. Because phase-X contains much larger amounts of potassium and water than coexisting phases in experimental products (e.g., diopside, garnet, and olivine), its abundance may be critical to the total amount of K and H_2O in a mantle assemblage. Consequently, we have determined the crystal structure to learn the K siting, the nature of the hydrous component as well as the general topology.

EXPERIMENTAL METHODS

Phase-X in the present study was produced at $P = 9$ GPa and $T = 1300$ °C from a mixture of natural diopside ($CaMgSi_2O_6$; with trace Al and Fe), synthetic kosmochlor ($NaCrSi_2O_6$), SiO_2, and $K_2CO_3 \cdot H_2O$ (approximate molar ratio 0.85:0.09:0.06:1), about 10 mg in total, sealed in a platinum capsule and placed in a multianvil device as experiment GG307 (see Harlow 1997 for synthesis details; note the pressure cited here reflects a newer calibration). Phase-X formed a thin layer (<100 μm thick) between clinopyroxene and quenched melt in the experiment. The crystals extracted from the experiment were embedded in epoxy and polished for electron microprobe analysis performed using a five-spectrometer Cameca SX100 electron microprobe. Standard compounds were natural diopside for Ca, Mg and Si, orthoclase for K and Al, $MgCr_2O_4$ for Cr, and jadeite for Na.

* The authors had requested that their paper appear with Yang et al. (2001).The Editors regret that this did not happen.

† E-mail: mancini@amnh.org

The extremely vulnerability of phase-X to electron beam damage at the initial analysis conditions of 15 kV and 10 nA beam current with a 2 μm beam diameter was evidenced by dark "burn" spots on analyzed grains and an oxide sum of only 85–86 wt%. Consequently the beam was enlarged to 20 μm diameter and current was lowered to 1 nA, which yielded no burn spot and an oxide sum of ~96 wt%. The average composition is presented in Table 1 and yields a chemical formula of $K_{1.03}Na_{0.05}(Mg_{0.92}Al_{0.03}Cr_{0.01})_2Si_{1.97}O_7H_{1.10}$ based on concurrence with Konzett and Fei (2000) for the requirement of structural water. Our phase-X is different from that synthesized by Konzett and Fei (2000) (see also Yang et al. 2001) in that it contains less K but measurable amounts of Cr and Al.

A small crystal was selected for X-ray diffraction after checking the sharpness of diffraction spots by precession camera and Mo$K\alpha$ (filtered) radiation. Diffraction intensities in a hemisphere of reciprocal space were measured on a Bruker P4 CCD Smart four-circle diffractometer with graphite monochromatized MoKa radiation at SUNY Stony Brook (see Table 2). The cell dimensions (Table 2) were precisely determined by the least-squares method, using the whole set of reflections with $|h| \le 6$, $|k| \le 6$, $|l| \le 16$. After a spherical absorption correction and merging of equivalent reflections, the data set consisted of 255 unique reflections ($I > 2\sigma$) that were used in the structure solution and refinement. Both the diffraction data from the precession camera and the CCD spots indicate systematic absence of reflections with l odd for $h\bar{h}0l$ suggesting the space groups $P6cc$, $P6_3cm$, or $P\bar{6}c2$, but consistent with a primitive hexagonal Bravais lattice.

The $|E^2-1|$ statistics for all unique reflections suggested the acentric space group $P6_3cm$ for structure solution. Direct methods (SHELXS–86, Sheldrick 1986) resulted in a structure model for the heavy atoms K, Si, and Mg and successive difference Fourier syntheses and Patterson method maps led to the positions of the O atoms. The refinement converged to R_u and R_w of 0.038 and 0.111, respectively for 138 unique reflections ($F_o > 4\sigma F_o$) after merging. All atoms in the structure occupy special positions (see Table 3). The K atom is surrounded by large lobes of residual electron density ±0.86 eÅ^{-3} on the Fourier map, so a split-site model was attempted. The refinement with K displaced to a general position (trigonal site splitting) converged at R_u and R_w of 0.017 and 0.051, respectively, which according to the significance tests on the crystallographic R factor (Hamilton 1965), is superior at the 0.005 level of significance. The final atomic coordinates are listed in Table 3 and apparent temperature factors in Table 4. In the last cycles of refinement, the scattering factors f' and f'' for ionized K were assigned to the 12d site and those for ionized Mg to the 4b site, and the site scatterings were refined (electrons per site, Table 3). The site scattering at 4b is consistent with an occupancy factor for Mg of 0.95 and minor Cr (0.02) and Al (0.03) occupancies, in agreement with the electron microprobe analysis (Table 1). The site scattering at 12d corresponds to an occupancy factor for K of 0.22.

IR spectra were collected on a second crystal of approximately the same size. The crystal was embedded in a 0.5 mm thick NaCl window and scanned through the 1100–6500 cm^{-1} region on a Nicolet 20SXB FTIR spectrophotometer linked to a Spectra-Tech IR plan microscope and equipped with a nitrogen-cooled InSb detector and a CaF_2 beam splitter; the nominal resolution is 4 cm^{-1} and final spectra are the average of 250 scans.

TABLE 1. Electron microprobe analysis (EPMA) of phase-X from experimental run GG307

Oxides (wt%)		Cations per 7O
SiO_2	45.906	1.968
Al_2O_3	1.360	0.069
Cr_2O_3	0.746	0.025
MgO	28.723	1.835
CaO	< d.l.	–
Na_2O	0.688	0.056
K_2O	18.765	1.026
*H_2O = OH	3.8	1.102
Total	99.97	6.081

Note: Detection limits: Na_2O, K_2O, SiO_2, CaO, MgO, Al_2O_3 = 0.01 wt%; Cr_2O_3 = 0.02 wt%.
* OH-content determined from charge balance.

TABLE 2. Crystal data and refinement information

Crystal size (μm)	20 × 20 × 30
Crystal color	yellow-green
Space group	$P6_3cm$ (no.185)
a (Å)	5.028(1)
b (Å)	5.028(1)
c (Å)	13.216(2)
α = γ (°)	90
β (°)	120
V (Å^3)	289.34
*Density (g/cm^3)	3.38
Wavelength (Å)	0.71070
Diffractometer	Bruker $P4$ 1K Smart CCD
Total exposures	1650
Scan mode Δω= Δφ (°)	0.3
T (K)	293
$2\theta_{max}$(°)	54.79
$hkl_{(total)}$	1521
$hkl_{(unique)}$	255
R_w	0.051
R	0.018

Note: The errors in parenthesis apply to the last digit.
* Density calculated assuming 100% occupancy.

DISCUSSION OF THE STRUCTURE

The structure of phase-X, Figures 1 and 2, is built up of octahedral sheets with dioctahedral character (2/3 of all edge-sharing octahedra created are filled) and layers consisting of pillars of disilicate groups [Si_2O_7] constructed of two non-equivalent SiO_4 tetrahedra. Within the [Si_2O_7] layer the potassium cations are accommodated in seemingly nine-fold coordination (A site) in the form of distorted trigonal antiprism. The alignment of these large trigonal cavities on [100], [010], and [110] directions produce channel structures. Each SiO_4 tetrahedron of the Si_2O_7 group shares edges with the A polyhedron and corners with the octahedral layer, above and below the vacant octahedron. Like the M octahedron, the A prism is centered on the threefold axis and shares basal triangular faces with the octahedron and quadratic lateral faces with other symmetrically related ones.

While the basic structure of phase-X was being deposited (Mancini et al. 2001), that of an anhydrous sodic phase-X was determined to have space group $P\bar{3}_1m$ (Yang et al. 2001). The major differences between the two structures as summarized in that study are (1) the octahedral stacking vectors between two neighboring octahedra that have the same orientation in $P\bar{3}_1m$, are instead reversed in $P6_3cm$, (2) the two equivalent tetrahedra in $P\bar{3}_1m$ eventually become non equivalent in $P6_3cm$,

TABLE 3. Atomic coordinates, refined site scatterings (e^-) and isotropic temperature factors ($Å^2$) of phase-X

Site	Position	Point symmetry	S_{ref}*	*x*	*y*	*z*	U_{eq}†
Si1	2*a*	3*m*	12	0	0	0.0127(3)	0.0089(7)
Si2	2*a*	3*m*	12	0	0	0.2602(2)	0.0046(6)
M	4*b*	3	12.68(7)	–0.3333	0.3333	0.1377(3)	0.0099(4)
K	12*b*	1	4.13(3)	0.3532(46)	0.6453(57)	0.3875(4)	0.0215(4)
O1	6*c*	*m*	8	0.3124(10)	0	0.2284(9)	0.0048(1)
O2	2*a*	3*m*	8.70(11)	0	0	–0.1110(20)	0.0162(9)
O3	6*c*	*m*	8	–0.3106(10)	0	0.0493(9)	0.0176(13)

Note: The errors in parenthesis apply to the last digit.
* S_{ref} = electrons per site.
† Form of the equivalent isotropic factor $U_{eq} = 8\pi^2\mu^2$.

TABLE 4. Anisotropic thermal parameters ($Å^2$) and bond valences (v.u.) of phase-X

Site	U_{11}	U_{22}	U_{33}	U_{23}	U_{13}	U_{12}	s
Si1	0.0102(10)	0.0102(10)	0.0065(14)	0	0	0.0051(5)	4.088
Si2	0.0069(9)	0.0069(9)	0.0001(12)	0	0	0.0034(4)	3.898
M	0.0080(4)	0.0080(4)	0.0137(5)	0	0	0.0040(2)	2.016
K	0.0153(46)	0.0239(66)	0.0082(6)	–0.0001(66)	0.0026(60)	–0.0030(16)	1.044*
O1	0.0051(16)	0.0035(19)	0.0052(24)	0	0.0005(23)	0.0017(9)	2.001
O2	0.0201(9)	0.0201(9)	0.0084(18)	0	0	0.0100(4)	2.018
O3	0.0153(18)	0.0201(23)	0.0190(27)	0	–0.0004(24)	0.0100(11)	1.977

Note: The error in parenthesis applies to the last digits.
* Bond valence sum calculated for five nearest bonded O atoms (see text).

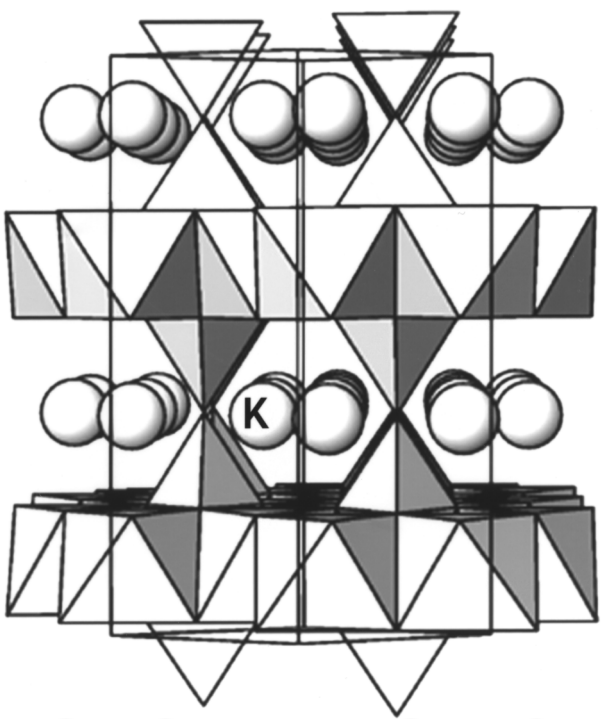

FIGURE 1. Three dimensional view of a slice of phase-X structure down [110]. Dioctahedral layer of MO_6 octahedra are linked by Si_2O_7 disilicate groups. The K atoms occupy a cavity connected by channels along [100], [110], and [010].

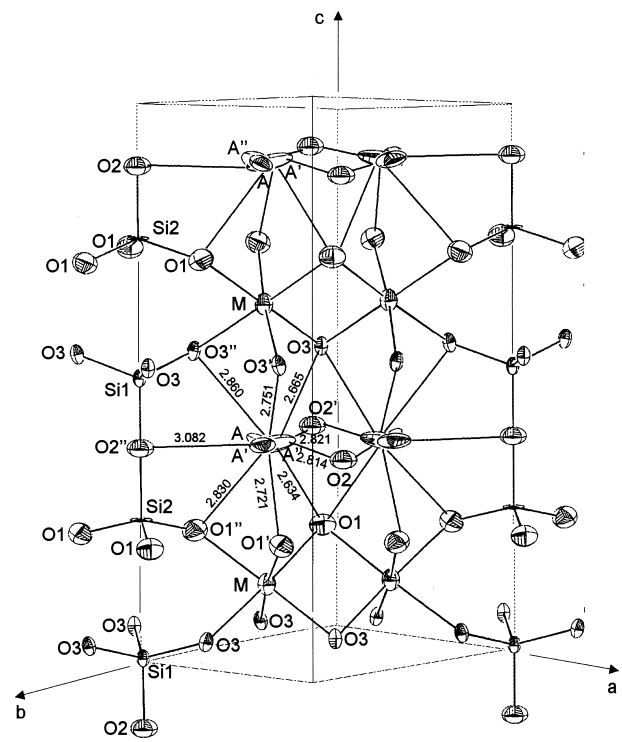

FIGURE 2. An ORTEP plot of a slice of the phase-X structures. Note the trigonal splitting of the A site (K position). Bond lengths are given in angstroms.

and (3) the two layers of O atoms in hexagonal closest packing that are equivalent in $P\bar{3}_1m$ become nonequivalent in $P6_3cm$.

Bond lengths are presented in Table 5. The Si2 tetrahedron is more distorted; it has three typical distances to basal O1 oxygen atoms, <Si2–O1> = 1.626 Å, but one distance to the bridging O2 atom, <Si2-$O2_{br}$> = 1.702 Å, which is longer than the mean Si-O_{br} for disilicates (Liebau 1985). Moreover, the Si1-Si2 distance, 3.30 Å, is long compared to the similar distance in sodium disilicate, 3.04 Å (Fleet and Henderson 1995, 1997). On the Fourier map, residual electron densities of 0.45 eÅ^{-3} at 0.70 Å from Si2 on the <Si2-$O2_{br}$> bond and of 0.43 eÅ^{-3} at 0.26 Å from O2 in the opposite direction are associated with σ (covalent) bonding (e.g., Sasaki et al. 1980; Fleet and Henderson 1995), as is a residual peak of 0.43 eÅ^{-3} at 0.76 Å from Si1 on the <Si1-$O2_{br}$> bond. As expected, the major axis of the vibrational ellipsoids of the bridging oxygen atom O2 is transverse to the <Si-O2> bonds ($U_{11} = U_{22} > U_{33}$; Table 4), a characteristic of disilicates (e.g., Fleet and Henderson 1995, 1997). The difference in mean-square displacement amplitudes between silicon and bridging O atoms calculated along the bonds (±0.0019 and ±0.0083 Å^2 for Si1-O2 and Si2-O2, respectively) are greater than predicted for a rigid covalent bond (i.e., ±0.001 Å^2, Downs et al. 1990 and references therein). However, in contrast to the nearly isotropic vibrational ellipsoid of the Si1 atom, that of Si2 is strongly flattened perpendicular to [001] (i.e., $U_{33} << U_{11}$, U_{22}; Table 4), indicating that Si2 is disordered on the *a-b* plane, possibly the result of different local atom configurations in the average structure (A site and/or H atom, see below). Attempts to refine a trigonal split model for Si2 were unsuccessful due to the small separation between potential subsites.

The M octahedron is nearly regular, being characterized by nearly equal M-O bonds (Table 5). The mean octahedral bond length, <M-O> = 2.098 Å, is slightly less than the sum of Mg (0.72 Å) and O (1.40 Å) ionic radii, consistent with the small but significant occupancies by Cr (0.02) and Al (0.03). Characteristically the octahedron possesses longer edges shared with adjacent octahedra (<O1-O3>$_{shr}$ = 3.023 Å and <O1-O3>$_{uns}$ = 2.838 Å; Table 5) opposite to most silicates (e.g., olivine, humite, pyroxene, amphibole, and mica) that invariably possess shorter shared edges due to strong cation-cation repulsion across the shared edges (Pauling 1947). This feature has also been observed in ringwoodite, <O-O>$_{shr}$ = 3.000 Å and <O-O>$_{uns}$ = 2.853 Å (Kudoh et al. 2000), and suggests a mechanism of densification that is effected largely by compression of the empty octahedron (e.g., Sinogeikin and Bass 1999).

The K atoms in the channel A site occupy any one of the three closely spaced split sites in each cavity (Fig. 2). The subsite is displaced 0.18 Å from the threefold axis and has the largest amplitude of the vibrational ellipsoid ($U_{22} > U_{11} >> U_{33}$; Table 4) in the K-K direction. This feature is similar to that in other high-pressure structures containing alkali ions disordered in channels sites (e.g., Vicat et al. 1986), suggesting that the displacement is in the direction of the next nearest (vacant) symmetric equivalent site, increasing the K-K separation between filled A sites and reducing the repulsive interactions. The cation displacement determines the distribution of K-O bonds and the five nearest "bonded" O atoms yield a total electrostatic charge to the K atom (using the formula of Brese and O'Keefe 1991) of +1.044 (Table 4). Noteworthy, the mean K-O interatomic distance of the tunnel A site ($^{[8]}$K-O = 2.76 Å) is significantly shorter than the sum of the ionic radii (2.95 Å), a contraction due to the partial occupancy. Likewise, a similar contraction is observed for the tunnel cation site of K-hollandite ($^{[8]}$K-O = 2.735 Å – Zhang et al. 1993).

The infrared spectrum of phase-X has a sharp absorption peak in the O-H stretching region at 3602 cm^{-1} (Fig. 3), suggesting the bulk OH^- structurally is bound in one anion site. Minor peaks are at 3410 and 4506 cm^{-1}; the latter, shallow and broader, could indicate Si-OH vibrations (e.g., Cordier and Doukhan 1991). As all anion sites in phase-X are directly bonded to Si atoms, such a vibration is likely and at least one tetrahedron must be acid in character. The nearly stoichiometric Si in the tetrahedral sites precludes a hydrogarnet-type $^{[4]}$Si ↔ 4H substitution (e.g., Lager et al. 1987), whereas the partial occupancy of the A site and requirements of electroneutrality imply the exchange H_xK_{-x}, via intersite atom-vacancy exchange $(K_{1-x}\square_x)^A \leftrightarrow (H_x\square_{1-x})^H$ although not on the A site alone. Bond-valence sums to O1 and O3—both coordinated to one Si atom, two M sites, and two A sites—are nearly ideal, 2.00 and 1.98 v.u. respectively (Table 4), and thus not suggestive as loci for H bonding. Turning to the bridging O atom, O2 is bonded to Si1 and Si2 and is surrounded by six nearest-neighbor A sites

TABLE 5. Selected interatomic distances, polyhedral volumes and distorsion indices of phase-X

Si1-O3	1.635(6)	*K"-O1	2.634(21)
Si1-O2	1.635(27)	K"-O1'	2.721(22)
Mean	1.635	K"-O1"	2.830(19)
Quad. elon. (λ)	1.001	K"-O2	2.814(20)
Angle vari. (σ_q)	5.888	K"-O2'	2.821(19)
V (Å^3)	2.234	K"-O2"	3.082(18)
Si2-O1	1.626(6)	K"-O3	2.665(21)
Si2-O2	1.702(26)	K"-O3'	2.751(22)
Mean	1.644	K"-O3"	2.860(21)
Quad. elon. (l)	1.005	Mean(8)	2.762
Angle vari. (σ_θ)	22.236	Mean(5)	2.717
V (Å^3)	2.264		
M-O1	2.105(7)		
M-O3	2.092(7)		
Mean	2.098		
Quad. elon. (λ)	1.002		
Angle vari. (σθ)	9.381		
V (Å^3)	12.281		

Note: The errors in parenthesis apply to the last digits.
*Atom symbols as in Figure 2.

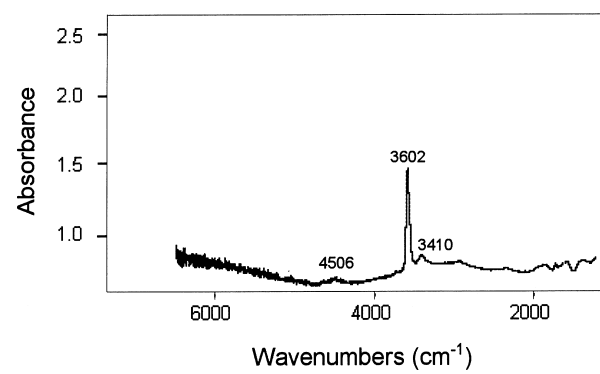

FIGURE 3. Non-polarized single-crystal FTIR spectra of phase-X in the 1250–6500 cm^{-1} region.

on the equatorial plane. Subtracting the bond valence contributions from Si1 (+1.01) and Si2 (+0.85) leaves 0.14 for other bonds if O2 is ideally saturated. This suggests that O2 is also coordinated to the closest K atom at 2.814 Å, which contributes 0.158 v.u., thereby yielding a total electrostatic valence of 2.018 v.u. Consequently, bond valence sums, like the Fourier maps, are inconclusive to the location of the H position. Because hydrous phase-X is acentric, it would make sense that O1 and O3 are different because of the preference of H for one or the other. The similar M-O1 and M-O3 distances do not preclude bonding to OH^-, as the modification of O atom by hydroxylation should not yield appreciable lengthening of the octahedral M-O bond (e.g., Gibbs et al. 1970), particularly in that only about one-third of either site would be affected. Alternatively, the distances to the tetrahedral cations, <Si1-O3> and <Si2-O1>, are respectively one normal and one short (above), unlike the relatively long <Si-O> bond that would result from $OH^- \leftrightarrow O^{2-}$ substitution (e.g., Lager et al. 1987). The bridging oxygen atom O2, which in the anhydrous form is constrained on the z = 1/2 mirror plane (Yang et al. 2001), is free to shift along the c-axis yielding a more "flexible" <Si-O_{br}> bond and is potentially able to eliminate overbonding from the H atom. In this light, an inclined O-H bond from the apical O atom toward the base of the Si2 tetrahedron could explain the relatively long <Si2-$O2_{br}$> and short <Si2-O1> distances as the result of Si-H repulsion. However, with the existing data no conclusion can be made on the location of H in phase-X.

The new structure of phase-X adds to the already known structures stable at high pressure in the K_2O-MgO-Al_2O_3-SiO_2-H_2O system (e.g., phlogopite, K-cymrite, K-hollandite, and KK-richterite) as a potential potassium- and water-bearing mantle mineral. Phase-X has some topological similarities to the structure of Na_2[6]Si[(4)Si_2O_7] (sodium trisilicate, Fleet and Henderson 1995, 1997) in which the octahedral and tetrahedral groups are linked together via shared corners. Densification of phase-X is largely created (1) by the greater compression of the empty octahedron and (2) by constraining the trigonal A cavity containing potassium to the size of an Si_2O_7 group.

Phase-X is another high-pressure silicate phase with partial vacancy on an alkali atom site in a large channel structure (i.e., K-hollandite and cymrite), possibly a result of the strong cation-cation repulsive interactions. Moreover, the vacancies in the large cavity provide another mechanism for structural accommodation to pressure. Resolution of these features of phase-X ultimately requires study at high pressure and temperature.

The composition of phase-X is not fixed but actually represents a solid solution in the stoichiometries $\square_2Mg_2Si_2O_7$-(K$\square$)$Mg_2Si_2O_7H$-$K_2Mg_2Si_2O_7H_2$, where the center part of the solid solution series appears to be the most stable portion at the conditions examined so far. Further examination of the limits to phase-X, including (Al,Cr) substitutions, is certainly in order. Also, as expected in a dense phase with most O atoms shared among all cations, the presenceOH necessarily requires the characterization of the phase as an acid silicate and begs a greater understanding of these rare forms of silicate.

ACKNOWLEDGMENTS

F.M. thanks H. Papunen, R. Sillanpää, and M. Sundberg for crystallographic advice as part of the Ph.D. program at the University of Turku (Finland). F.M. acknowledges support from an AMNH fellowship, and G.E.H. gratefully acknowledges support through NSF grants EAR-9314819 and EAR-9903203.

REFERENCES CITED

Brese, N.E. and O'Keefe, M. (1991) Bond-valence parameters for solids. Acta Crystallographica, B47, 192–197.

Cordier, P. and Doukhan, J.C. (1991) Water speciation in quartz: a near infrared study. American Mineralogist, 76, 361–369.

Downs, R.T., Gibbs, G.V., and Boisen, M.B., Jr. (1990) A study of the mean-square displacement amplitudes of Si, Al, and O atoms in framework structures: Evidence for rigid bonds, order, twinning, and stacking faults. American Mineralogist, 75, 1253–1267.

Fasshauer, D.W., Chatterjee, N.D., and Marler, B. (1997) Synthesis, structure, thermodynamic properties, and stability relations of K-cymrite, $K[AlSi_3O_8]\cdot H_2O$. Physics and Chemistry of Minerals, 24, 455–462.

Fleet, E.M. and Henderson, G.S. (1995) Sodium trisilicate: a new high-pressure silicate structure ($Na_2Si[Si_2O_7]$). Physics and Chemistry of Minerals, 22, 383–386.

———(1997) Structure-composition relations and Raman spectroscopy of high-pressure sodium silicates. Physics and Chemistry of Minerals, 24, 345–355.

Gibbs, G.V., Ribbe, P.H., and Anderson, C.P. (1970) The crystal structure of the humite minerals. II. Chondrodite. American Mineralogist, 55, 1182–1194.

Hamilton, W.C. (1965) Significance tests on the crystallographic R factor. Acta Crystallographica, 18, 502–510.

Harlow, G.E. (1997) Potassium in clinopyroxene at high pressure and temperature: An experimental study. American Mineralogist, 82, 259–269.

Inoue, T., Irifune, T., Yurimoto, H., and Miyagi, I. (1998) Decomposition of K-amphibole at high-pressure: implications for subduction zone volcanism. Physics of the Earth and Planetary Interiors, 107, 221–231.

Irifune, T., Ringwood, A.E., and Hibberson, W.O. (1994) Subduction of continental crust and terrigenous and pelagic sediments: an experimental study. Earth and Planetary Science Letters, 77, 351–368.

Konzett, J. and Fei, Y. (2000) Transport and storage of potassium in the Earth's upper mantle and transition zone: an experimental study to 23 GPa in simplified and natural bulk compositions. Journal of Petrology, 41, 583–603.

Kudoh, Y., Kuribayashi, T., Mizobata, H., and Ohtani, E. (2000) Structure and cation disorder of hydrous ringwoodite, γ-$Mg_{1.89}Si_{0.98}H_{0.30}O_4$. Physics and Chemistry of Minerals, 27, 474–479.

Lager, G. A., Armbruster, T., and Faber, J. (1987) Neutron and X-ray diffraction study of hydrogarnet $Ca_3 Al_2 (O_4 H_4)_3$. American Mineralogist, 72, 756–765.

Liebau, F. (1985) *Structural chemistry of silicates.* Springer-Verlag, Berlin.

Luth, R.W. (1997) Experimental study of the system phlogopite-diopside from 3.5 to 17 GPa. American Mineralogist, 82, 1198–1209.

Mancini, F., Harlow, G.E., and Cahill, C.L. (2001) Crystal structure of potassium dimagnesium dislicate hydroxide, $K_{1.3}(Mg_{0.95}Al_{0.03}Cr_{0.02})_2Si_2O_{6.4}(OH)_{0.6}$. Zeitschrift für Krystallographie, NCS 216, 189–190.

Pauling, L. (1947) The Nature of the Chemical Bond, 2nd ed., 72 p. Cornell University Press, Ithaca, New York.

Sasaki, S., Fujino, K., Takeuchi, Y., and Sadanaga, R. (1980) On the estimation of atomic charges by the X-ray method for some oxides and silicates. Acta Crystallographica, A36, 904–915.

Schmidt, M.W. (1996) Experimental constraints on recycling of potassium from subducted oceanic crust. Science, 272, 1927–1930.

Sheldrick, G.M. (1986) SHELXS-86. Program for Crystal Structure Solution. University of Göttingen, Germany 1986.

Sinogeikin, S.V. and Bass, J.D. (1999) Single-crystal elastic properties of chondrodite: implication for water in the upper mantle. Physics and Chemistry of Minerals, 26, 297–303.

Thompson, P., Parsons, I., Graham, C., and Jackson, B. (1998) The breakdown of potassium feldspar at high water pressures. Contributions to Mineralogy and Petrology, 130, 176–186.

Trønnes, R.G. (1990) Low-Al, high-K amphiboles in subducted lithosphere from 200–400 Km depth: experimental evidence. EOS Transactions, 71, 1587.

Ulmer, P. and Konzett, J. (1999) The stability of hydrous potassic phases in lherzolitic mantle—an experimental study to 9.5 GPa in simplified and natural bulk compositions. Journal of Petrology, 40, 629–652.

Vicat, J., Fanchon, E., Strobel, P., and Tran Qui, D. (1986) The structure of $K_{1.33}Mn_8O_{16}$ and cation ordering in hollandite-type structures. Acta Crystallographica, B42, 162–167.

Yamada, H., Matsui, Y., and Ito, E. (1984) Crystal-chemical characterization of $KAlSi_3O_8$ with the hollandite structure. Mineralogical Journal, 12, 29–34.

Yang, H., Konzett, J., and Prewitt, C.W. (2001) Crystal structure of a new (21)-clinopyribole synthesized at high temperature and pressure. American Mineralogist, 86, 1261–1266.

Zhang, J., Ko, J., Hazen, R., and Prewitt, C.W. (1993) High-pressure crystal chemistry of $KAlSi_3O_8$ hollandite. American Mineralogist, 78, 493–499.

MANUSCRIPT RECEIVED APRIL 3, 2001
MANUSCRIPT ACCEPTED NOVEMBER 7, 2001
MANUSCRIPT HANDLED BY JAMES W. DOWNS